Biol Cybern (2014) 108:291–303
DOI 10.1007/s00422-014-0592-8

ORIGINAL PAPER

Biological Cybernetics

Multi-layered multi-pattern CPG for adaptive locomotion of humanoid robots

John Nassour · Patrick Hénaff · Fethi Benouezdou · Gordon Cheng

Received: 8 May 2013 / Accepted: 3 February 2014 / Published online: 26 February 2014

Abstract In this paper, we present an extended mathematical model of the central pattern generator (CPG) in the spinal cord. The proposed CPG model is used as the underlying low-level controller of a humanoid robot to generate various walking patterns. Such biological mechanisms have been demonstrated to be robust in locomotion of animal. Our model is supported by two neurophysiological studies. The first study identified a neural circuitry consisting of a two-layered CPG, in which pattern formation and rhythm generation are produced at different levels. The second study focused on a specific neural model that can generate different patterns, including oscillation. This neural model was employed in the pattern generation layer of our CPG, which enables it to produce different motion patterns—rhythmic as well as non-rhythmic motions. Due to the pattern-formation layer, the CPG is able to produce behaviors related to the dominating rhythm (extension/flexion) and rhythm deletion without rhythm resetting. The proposed multi-layered multi-pattern CPG model (MLMP-CPG) has been deployed in a 3D humanoid robot (NAO) while it performs locomotion tasks. The effectiveness of our model is demonstrated in simulations and through experimental results.

Keywords Central pattern generator · Robot locomotion · Humanoid walking

1 Introduction

The coordination of body movements plays an important role in keeping animals alive and helping them explore their environments (Purves et al. 2004). Local circuits (central pattern generators) have been identified in the spinal cords of vertebrates as responsible for locomotor movements (Brown 1914).

More specifically, the central pattern generator (CPG) is a set of interneurons and motor neurons located in the spinal cord, which can generate patterns without sensory feedback. These neurons locally control the sequence of contraction and relaxation of muscles. However, sensory feedback is essential to shape the generated motion patterns. Meanwhile, descending signals from the higher centers contribute to the synchronization between patterns and also to the modulation of the CPG neurons. The sensory neurons provide proprioceptive and exteroceptive feedback. In the proprioceptive loop, they detect the stretching and the contraction of muscles. They can also provide sensory information, such as internal forces or articular positions. In the exteroceptive loop, sensory neurons detect interactions with the environment like the contact between the foot and the ground. All sensory neurons act directly or through interneurons to modulate signals gener-

Electronic supplementary material The online version of this article (doi:10.1007/s00422-014-0592-8) contains supplementary material, which is available to authorized users.

J. Nassour (✉) · G. Cheng
Institute for Cognitive Systems (ICS),
Technical University of Munich (TUM), Munich, Germany
e-mail: nassour@tum.de

G. Cheng
e-mail: gordon@tum.de
URL: http://www.ics.ei.tum.de

P. Hénaff
LORIA, UMR 7503, University of Lorraine-INRIA-CNRS,
University of Lorraine, F-54506 Nancy, France
e-mail: patrick.henaff@univ-lorraine.fr

F. Benouezdou
The Engineering System Laboratory (LISV),
Versailles University (UVSQ), Versailles, France
e-mail: Fethi.Benouezdou@uvsq.fr

ated by rhythmic neurons or motor neurons. The three types of the above-mentioned neurons are also involved in reflexive responses to stimuli. The higher centers of the brain are also involved in locomotion by controlling the spatial and temporal activity patterns of individual limbs (Rossignol et al. 2006). However, it has been demonstrated that a cat's hindlimbs can produce walking patterns even with a cut to the spinal cord at the thoracic level (Purves et al. 2004; Shik et al. 1966).

1.1 Neurobiological studies

Neurobiological studies on decerebrate cats have proposed computational models of spinal circuitry responsible for animal locomotion (Brown 1911; Orlovsky et al. 1999; Rybak et al. 2006; McCrea and Rybak 2008). Rhythmic patterns in cat limbs are generated in the absence of signals from higher centers and are able to control the timing and the coordination of limbs' motion depending on the lesion level (Brown 1911; Orlovsky et al. 1999). Each joint appears to have its own CPG, which can be coupled to the CPG of another joint to produce complex movements. These CPGs controlling such behaviors in animals' locomotion may also be responsible for rhythmic movements in human locomotion (Choi and Bastian 2007).

Several schemes for the spinal CPG have been proposed to generate rhythmic movements: "half-center CPG" was proposed by Brown (1914), "half-center CPG" with more complex patterns of motoneuron activity was introduced by Perret et al. (1988), and "half-center CPG" with sensory input was proposed by Orlovsky et al. (1999).

Due to the direct excitatory connection between the rhythm-generation interneurons and the motoneurons, the single-level CPG models are unable to show the robust behaviors observed in animals' locomotion: even a short absence of the rhythmic signals would affect the cycle timing and the phase of the pattern (Rybak et al. 2006; McCrea and Rybak 2008). For instance, when walking up or down inclined terrain, any change in the excitability of the half-centers affects both cycle timing and motoneuron activity, while an independent regulation of these parameters is required. The association of cycle timing and motoneuron activity requires a more complex architecture than the single-level CPG.

This more sophisticated architecture is required to manage the adaptation to environmental changes. Therefore, two- and three-layered CPGs with rhythm-generation and pattern-formation circuitry have been proposed in Rybak et al. (2006); McCrea and Rybak (2008) and Koshland and Smith (1989). These models separate cycle timing and motoneuron activation during locomotion. The CPG model proposed by Rybak et al. (2006) is a model with two layers, composed of a half-center rhythm generator (RG) that controls the rhythm and duration of extension and flexion phase of muscles, and a pattern-formation (PF) interneuron layer that excites motoneuron (MN) populations and inhibits other PF populations. The PF layer distributes rhythmic inputs from the RG network among the motoneuron pools. Activation of a particular PF population will activate the corresponding motoneuron population and thus activate the corresponding muscle. Afferent feedback may affect the CPG at the RG layer; this can produce alterations in the generated locomotor rhythm in terms of phase shifting or phase resetting. If the effect of the afferent feedback occurs at the pattern-formation layer, it may affect the activation and timing of the phase transition without inducing phase shifting or resetting. Reflex circuitry is defined by the connections between afferent feedback and motoneuron populations (e.g., stretch reflex and flexion reflex).

1.2 Biomechanical studies

Apart from neural-based studies, biomechanical studies have found that locomotion can also be produced with a simple state machine that encodes the principles of legged mechanics to produce walking behaviors similar to those of humans. The muscle-reflex model proposed by Geyer and Herr (2010) was tested on a two-dimensional human lower body model in simulation to achieve walking. However, this approach requires designing new rules for any additional behaviors. Unlike biomechanics models, where the main focus is matching the locomotor behavior to the biomechanical data, neural-based techniques for robot locomotion are interested furthermore in minimizing the number of the required parameters and in the generalization of the proposed circuitry to multiple locomotor behaviors.

1.3 CPG and robot locomotion

Several neural-based models have been proposed previously for robot locomotion (Taga et al. 1991; Miyakoshi et al. 1998; Ijspeert et al. 2007). In those studies, sensory feedback has been used to manage the dynamic interaction of the environment with the generated rhythmic activities of the neural controller, composed of coupled neural oscillators, and the rhythmic movements of a musculo-skeletal system (Taga et al. 1991). Other neural-based models generate walking patterns only from the interaction with the ground (Manoonpong et al. 2007). Miyakoshi et al. constructed a neural oscillator system to generate walking patterns that ensures a stable stepping motion under perturbation (Miyakoshi et al. 1998). Many of these previous models have been shown to be able to address certain environmental changes during periodic walking. However, they do not account for actions that require a non-rhythmic motion, such as sudden motion changes, such as push recovery. Ijspeert has shown phase transition between walking activity and swimming activity of his salamander

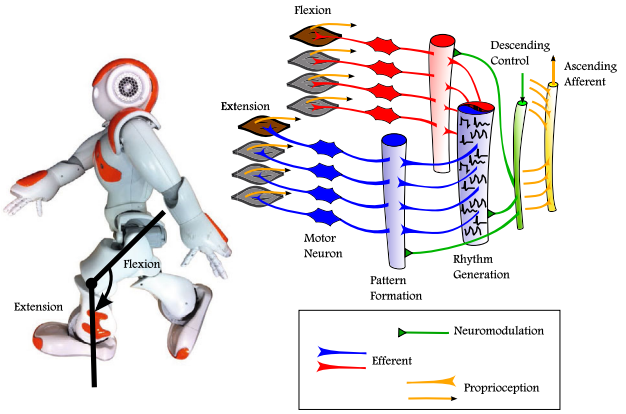

Fig. 1 Conceptual overview of the multi-layer multi-pattern CPG for humanoid robot locomotion

robot driven by a spinal cord model (Ijspeert et al. 2007). The combination of discrete and rhythmic motor primitives of a central pattern generator has been presented by Degallier et al. (2011), where discrete movements are obtained by setting the oscillators' amplitude to zero and including a constant offset. So far, the existing neural-based motion pattern generators consider the discrete and rhythmic movements separately, without a unique diverse pattern generator.

This paper proposes a CPG model that can generate different motion patterns by varying only a small number of parameters. We present a multi-layered, multi-pattern CPG that can exhibit a wide variety of patterns and different possibilities to control these patterns to generate walking behaviors and even abrupt reactions. Our proposed CPG model is validated in simulations and experiments on a NAO humanoid robot (see Fig. 1). Section 2 describes the architecture and the neural model of each layer of the CPG. The observed behaviors at the joint level are presented in Sect. 3. Section 4 details the entire architecture for humanoid robot locomotion. The robustness of the proposed model for walking on sloped terrain and also in reaction to external perturbation force is shown in Sect. 5. We conclude with a discussion of the presented model.

2 The multi-layered multi-pattern CPG model

This section first presents the architecture of one joint for the proposed CPG model. Then, neural models are detailed for each layer and for sensory neurons.

2.1 MLMP-CPG architecture

Similar to that in biological systems, a computational model of a CPG must be able to receive tonic drive from the high-level controller (for instance, supraspinal locomotion centers in mammals) (Markin et al. 2010). The mesencephalic locomotor region (MLR) is one of the locomotion control centers in the brainstem and was discovered in cats by Shik et al. (1966). The descending drive signal from the MLR allows the CPG to generate basic locomotor behaviors by providing alternating activation of the corresponding motoneurons that drive joint actuators (extensor and flexor muscles). Figure 2 shows the proposed basic CPG wiring diagram for one robot joint after merging two neurophysiological studies (Rybak et al. 2006; Rowat and Selverston 1991). The architecture of the CPG is based on the work of Rybak et al. for a two-level CPG that separates the timing and activation of the locomotion cycle (Rybak et al. 2006); the neural model responsible for the generated behavior is proposed by Rowat and Selverston (1991) and can generate both rhythmic and non-rhythmic activation.

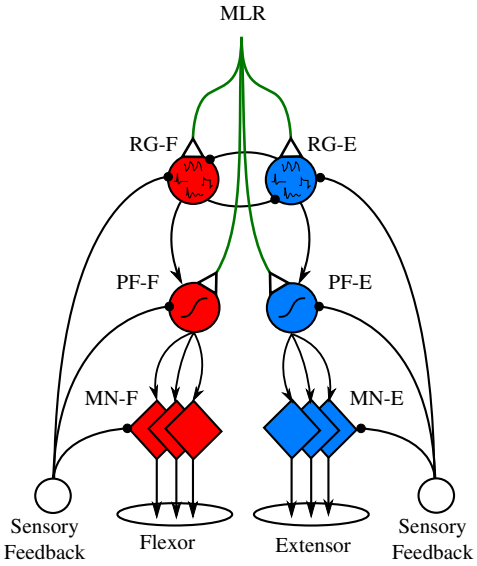

Fig. 2 Model of one joint CPG controller with three layers: rhythm generator (RG), pattern-formation (PF), and motoneuron (MN) layer

The proposed CPG architecture is separated into three layers: (i) rhythm-generation neurons (RG); (ii) pattern-formation neurons (PF); and (iii) motoneurons (MN). In the rhythm-generation layer, different types of patterns can be generated, including the rhythmic ones. The pattern-formation layer is responsible for shaping the generated patterns, and it controls which rhythm dominates for the corresponding joint (extension/flexion). Sensory neurons (feedback) shape the activity of the CPG neurons. The following subsections introduce each of these layers.

2.2 Model of rhythmic generator neurons

In animal locomotion, the control of the musculoskeletal system is ensured in a hierarchical manner by a high-level nervous system and spinal cord nervous system (CPG) for rhythmic locomotion patterns. Several mathematical models

have been proposed for rhythmic pattern generation [e.g., Matsuoka (1985), Taga et al. (1991), Rowat and Selverston (1991)], and some of these have been implemented in the locomotion of legged robots (Endo et al. 2004; Righetti and Ijspeert 2006; Ijspeert et al. 2007; Endo et al. 2008).

Among many models of neural-based motor pattern generators, the Matsuoka oscillator is widely used in robotics research. The Matsuoka model is based on the mutual inhibition of two neurons with self-inhibition effect. Based on these connections, each neuron can produce rhythmic activity. Taga et al. used the Matsuoka oscillator as a neural rhythm generator to control the locomotion of a bipedal robot in a 2D simulated environment (Taga et al. 1991). Their controller is based on the Matsuoka model as a unit oscillator, producing a torque to be applied on a specific joint. The Matsuoka model has been widely used in legged robots' locomotion to generate walking patterns (Endo et al. 2004; Matsubara et al. 2006; Liu et al. 2008). In Matsuoka and Taga's models, the oscillatory behavior arises from the mutual connection between neurons; however, neither neuron can produce an oscillatory activity without coupling with another neuron (Endo et al. 2008). Furthermore, the Matsuoka model is limited only oscillatory patterns (Liu et al. 2007), but complex behavioral motion requires a combination of multiple motor behaviors. Another neural model must be employed in robot locomotion to show complex motions while interacting with the surrounding world.

Rowat and Selverston proposed a neural model based on two cells with self-rhythmic generation ability (Rowat and Selverston 1997). Each cell independently generates its own pattern according to two parameters that are related to the membrane conductivities for fast and slow currents. All fast membrane currents are represented by a single fast current, and all slow membrane currents are represented by a single slow current. This model is represented by two differential equations:

$$\tau_m . \frac{\mathrm{d}V}{\mathrm{d}t} = -(\mathrm{fast}(V, \sigma_f) + q - i_{\mathrm{inj}}) \tag{1}$$

$$\tau_s . \frac{\mathrm{d}q}{\mathrm{d}t} = -q + q_\infty(V) \tag{2}$$

$$\tau_m < \tau_s \tag{3}$$

Here, V is the membrane potential, and q is the lumped slow current. While the fast current is supposed to activate immediately, the membrane time constant τ_m is assumed to be significantly smaller than the slow current's time constant for activation τ_s. The ratio of τ_s to τ_m was fixed at 20 in Rowat and Selverston (1997), but when the ratio is as small as 1.5 , most model patterns still arise. The injected current is i_{inj}. An idealized current–voltage curve for the lumped fast current is given by the following equation:

$$\mathrm{fast}(V, \sigma_f) = V - A_f \tanh((\sigma_f / A_f) V) \tag{4}$$

The fast current represents the sum of a leak current and an inward Ca^{++} current. The dimensionless shape parameter for the current–voltage curve is given by the following equation:

$$\sigma_f = \frac{g_{Ca}}{g_L} \tag{5}$$

Here, g_L is the leak conductance, and g_{Ca} is the calcium conductance. $q_\infty(V)$ is the steady-state value of the lumped slow current, which is given by the following equation:

$$q_\infty(V) = \sigma_s (V - E_s) \tag{6}$$

$q_\infty(V)$ is linear in V with a reversal potential E_s. σ_s is the potassium conductance g_K normalized to g_L. σ_s is given by:

$$\sigma_s = \frac{g_K}{g_L} \tag{7}$$

This model can be extended to show two different conductances for inward and outward, with conductance σ_{in} for inward slow current smaller than for outward slow current σ_{out}. The steady-state value of the lumped slow current is given by the following equation:

$$q_\infty(V) = \begin{cases} \sigma_{\mathrm{in}}(V - E_s) & \text{if } V < E_s \\ \sigma_{\mathrm{out}}(V - E_s) & \text{if } V > E_s \end{cases} \tag{8}$$

q and i_{inj} have the dimension of an electrical potential. A true current is obtained by multiplying the model current by the leak conductance, g_L. V, E_s, i_{inj}, and q are given in millivolts, while τ_s and τ_f are expressed in milliseconds.

With different values of the cell parameters, different intrinsic patterns can be generated: quiescence (Q), almost an oscillator (A), endogenous oscillator (O), plateau (P), depolarization (D), and hyperpolarization (H), as shown in Fig. 3. According to Rowat and Selverston (1997), the most influential parameters are σ_s, σ_f, and i_{inj}.

Rowat and Selverston's cell model was used in robotic locomotion to design a controller for a multi-legged robot (Hoinville 2007). This work showed that such a neural model is very well suited to generating adaptive rhythmic locomotion for multi-legged robots because it demonstrated properties of plasticity through its parameters. This cell model has been shown to be effective at controlling a two-joint planar simulated leg that slips on a rail, demonstrating the role of

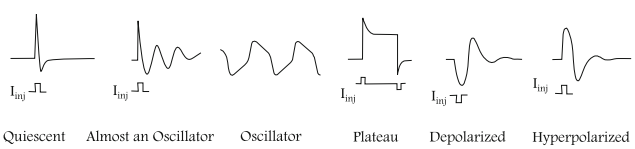

Fig. 3 The six intrinsic patterns of the cell's model, Rowat and Selverston (1991). These patterns are very similar to the four rhythms described in Marder and Bucher (2001): Endogenous bursting, Postinhibitory rebound, Plateau potentials, and Spike frequency adaptation

sensory feedback on a CPG model to improve the locomotion task (Amrollah and Henaff 2010).

2.3 Model of pattern-formation neurons

Neurons at this layer have inputs from the rhythm-generation layer and inputs from proprioception and exteroception. In neurophysiological studies, it has been shown that the pattern-formation neurons also have a supraspinal driver that modulates the functionality of PF neurons not to change the activation rhythm, but rather to balance between flexion domination and extension domination (Rybak et al. 2006). The supraspinal drive to pattern-formation neurons ensures rhythm deletion of motoneurons activities without resetting the phase in the rhythm-generation layer (e.g., RG neurons continue oscillating, while motoneurons are not active). Ryback et al. observe a deletion of the generated rhythm during animals' locomotion; however, muscles are able to return to the previous rhythm. This is described as "rhythm deletion without phase resetting" (Rybak et al. 2006). Although the motoneuron output (extensor, flexor, or both) was absent for a while, the original oscillation (rhythm) is preserved even after the deletion.

We propose a model for pattern-formation neurons that considers the biological inspiration related to rhythm domination and deletion and the brainstem descending control into pattern-formation neurons (McCrea and Rybak 2008). Two key parameters that control the amplitude of the activation of the neuron and the saturation were considered. In this study, we use the Sigmoid as an activation function of pattern-formation neurons. Therefore, the activation value of the neuron will be modulated by changing the slope of the Sigmoid and also the central point of the curve. However, any other activation function that considers these control keys will also be applicable. The activation function of pattern-formation neurons in this study is calculated as follows:

$$\mathrm{PF}_i = \frac{1}{1 + e^{\alpha.\alpha_{\mathrm{MLR}}((\theta+\theta_{\mathrm{MLR}})-I)}} \tag{9}$$

$$I = \frac{w_{\mathrm{rg}\to\mathrm{pf}}.\mathrm{RG}_i + \sum_{j=1}^{n} w_j.S_j}{n+1} \tag{10}$$

Here, PF_i is the activation value of the i^{th} pattern-formation neuron, α is a single value that denotes the slope of the Sigmoid function, θ is the center point of the curve that denotes the threshold of the neuron, I is the average input to pattern-formation neurons, $w_{\mathrm{rg}\to\mathrm{pf}}$ is the weight of the synaptic connection between rhythm-generation neurons and pattern-formation neurons, RG_i is the activation of the ith rhythm generator neuron, S_j is the activation of the *proprioception* or *exteroception* neuron, and w_j is the weight between this neuron and the pattern-formation neuron. α_{MLR} is a single value that represents the descending control from the high-level controller to modulate the activation of the neuron regarding the input range of the pattern-formation neuron. θ_{MLR} is the modulation of the threshold by the high-level controller that drives the rhythm domination (extension/flexion). Figure 4 shows the activation function of a pattern-formation neuron with different descending control values.

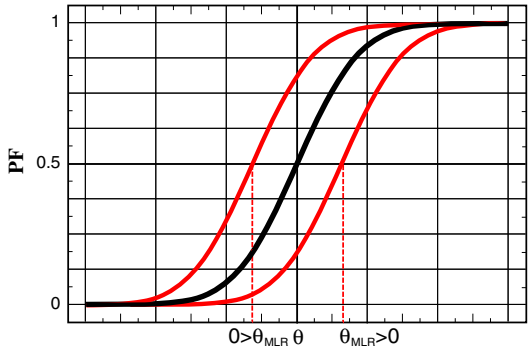

(a) The neuromodulation of the center point of the curve of the activation function of pattern-formation neurons.

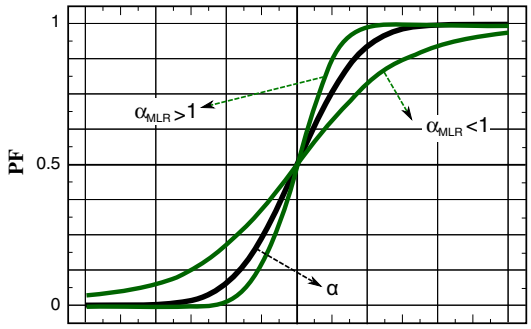

(b) The neuromodulation of the slope of the curve of the activation function of pattern-formation neurons.

Fig. 4 Effects of the descending control from higher centers on the activation function of pattern-formation neurons. Black lines correspond to $\theta_{\mathrm{MLR}} = 0$ in **a** and $\alpha_{\mathrm{MLR}} = 1$ in **b**

2.4 Model of motor neurons

The activation of motoneurons is calculated as follows:

$$\mathrm{MN}_i = \frac{1}{1 + e^{\alpha(\theta - I)}} \tag{11}$$

$$I = \frac{w_{\mathrm{pf}\to\mathrm{mn}}.PF_i + \sum_{j=1}^{n} w_j.S_j}{n+1} \tag{12}$$

Here, α and θ are the slope and the threshold of the Sigmoid activation function. In this paper, they are fixed empirically at 5 and 0.5, respectively. I denotes the average input to motoneurons. S_j is the activation of the related sensory neuron, and w_j is the weight between this neuron and the corresponding motoneuron. $w_{\mathrm{pf}\to\mathrm{mn}}$ is the weight of the synaptic connection between pattern-formation neurons and motoneurons.

2.5 Model of sensory neurons

A static model of a sensory neuron proposed by Wadden and Ekeberg (1998) is described in Eq. (13). ρ_i is the activity of sensory neuron, α is a positive constant that denotes the dynamics of the neuron, θ is the mid-range input, and ϕ is the input to the neuron. ϕ can be an angular position or a contact force (Geng et al. 2006).

$$\rho_i = \frac{1}{1 + e^{\alpha(\theta - \phi)}} \tag{13}$$

The extension and flexion sensory neurons in each joint (ES and FS) inhibit the corresponding motoneuron for this joint. This circuitry is described as articular reflex. ES and FS sensory neurons for each joint have similar thresholds calculated as follows: $\theta = (\phi_{\max} + \phi_{\min})/2$, where ϕ represents the joint's angle. ES and FS sensory neurons have slopes α with different signs, one with positive and the other with negative slope. The values of α are selected in the way that ensures variation of at least 90 % in the output of sensor neurons when the input (the joint's angle) changes between $\phi_{\min}$ and $\phi_{\max}$.

3 MLMP-CPG behaviors

Our CPG model has two control levels. The first level concerns the generated rhythm, and the second level concerns the pattern shape. By controlling CPG on these levels, our model can generate different locomotor behaviors. We distinguish two categories of behaviors: the first is related to the rhythm-generation layer, and the second is related to the pattern-formation layer.

3.1 Rhythm generation

After observing the phase diagram of a joint and changing the parameters σ_s and σ_f in the rhythm generator neurons, different motion behaviors were observed. Based on metric $\mathcal{E}$ (see Eq. 14), which reflects the kinetic energy, patterns were classified.

$$\mathcal{E} = \int_{t_0}^{t_f} \dot{\theta}^2 \, \mathrm{d}t \tag{14}$$

Here, $\dot{\theta}$ is the angular velocity of the joint. Figure 5 shows the distribution of the four *basic* motion patterns in space of σ_s and σ_f. Altering σ_s and σ_f allows neurons to exhibit different activities. Furthermore, the variation in the amplitude of the injected current i_{inj} will lead the neuron to produce additional patterns, as presented in Fig. 3. However, this paper address only the variation in the space of σ_s and σ_f. The basic behaviors presented in Fig. 5 could lead the robot

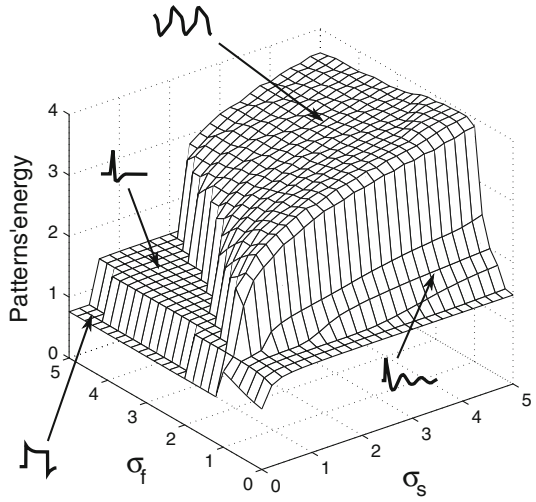

Fig. 5 The different basic behaviors observed on the joint for the same injected current: distribution of these motion patterns in space of σ_s and σ_f. The four behaviors are Plateau, Quiescent, Almost an oscillator, and Oscillatory behavior

to achieve complex tasks, such as walking in different conditions and reacting to sudden external disturbances. Motions with *plateau* behaviors have the lowest values for the energy-based metric, followed by motions with *Quiescent* behaviors, then motions with *Almost an Oscillator*, and then oscillatory behaviors that have the highest values for the energy-based metrics. Therefore, all motion behaviors can be classified on a new axis according to energy reference. They are positioned on the axis as follows: *Plateau, Quiescent, Almost an oscillator, and Oscillatory* motion. Two-dimensional space (σ_s, σ_f) is represented in only one-dimension axis, and one axis is needed for each joint to illustrate all its motion patterns (see the illustration in Fig. 12).

3.2 Pattern formation

Patterns generated by RG neurons are transmitted into motor neurons by the pattern-formation layer, where they are shaped according to external or internal variables. This control level explains the non-resetting deletion behaviors that have been observed in animal locomotion (Lafreniere-Roula and McCrea 2005) (deletion without resetting the rhythm).

Furthermore, it also explains extensor and flexor domination. The role of the pattern-formation layer is detailed in McCrea and Rybak (2008). Figure 6 shows the effect of extensor and flexor domination on a generated oscillatory motion for one joint. The activation of the CPG neurons is illustrated for extensor domination and flexor domination with and without feedback. Extensor-dominated motion was achieved with the descending control $\theta_{\text{MLR}} = +0.5$, and flexor-domination motion was achieved with the descending control $\theta_{\text{MLR}} = -0.5$. The variation in θ_{MLR} changes the

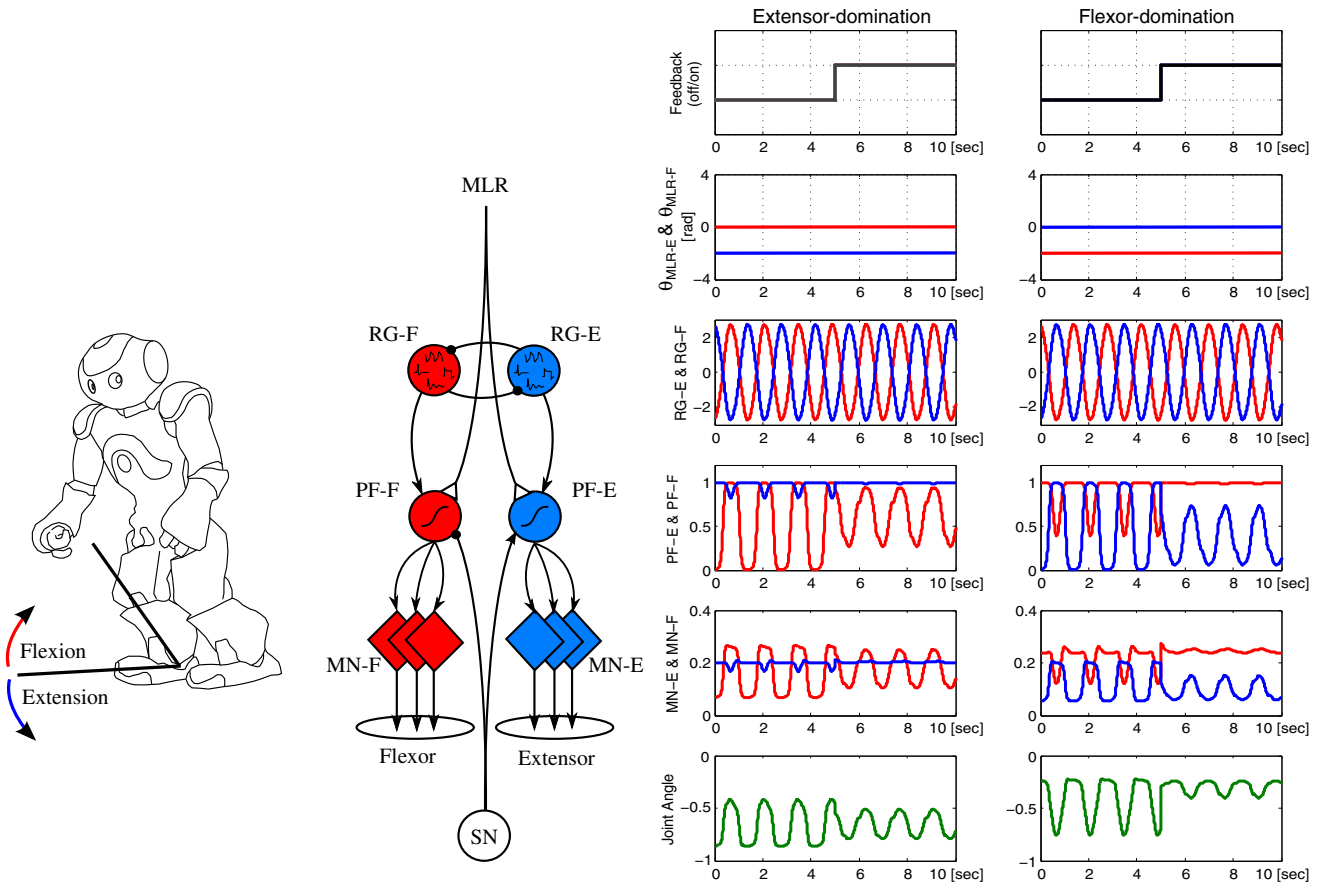

Fig. 6 Neural activation of one joint CPG during extensor-dominated rhythm and flexor-dominated rhythm with and without the feedback from the sensory neuron (SN). The activities of neurons in flexion side are referred by red curves. The activities of neurons in extension side are referred by blue curves. The descending control θ_{MLR} drives the behavior of the CPG between extensor and flexor domination

behavior of the CPG to show extensor or flexor domination behavior, which brings a certain robustness to environmental changes.

4 MLMP-CPG for humanoids

This section introduces the complete architecture of the CPGs to generate diverse patterns for humanoid robot locomotion. It precisely describes the inter- and intra-limb coordination, and details the CPG circuitry for each joint. The role of phase resetting in the stability for robot walking on flat terrain is also presented.

4.1 Motor coordination

There are several areas of the brain that are involved in temporal coordination of the limbs (Swinnen et al. 2010). According to Haken et al. (1985), motor coordination can be modeled as coupled oscillators. Based on these studies, we suggest that the inter-joint coordination circuitry is task-related (i.e., different couplings for different tasks) and can be defined by a descending motor program from a high-level controller. Figure 7 shows the proposed inter-joint coordination circuitry between the CPGs for each joint of the NAO humanoid robot. This circuitry was designed manually to produce the walking behavior. The coordination occurs on the layer of rhythm-generating neurons.

The principle of our proposed circuit for walking is described by the activity between the CPGs, which is regulated by excitatory synaptic connections. For inter-limb circuitry, the rhythm-generating extensor neuron in the left hip pitch (E-LH-P) excites the rhythm-generating flexor neuron in the right hip pitch (F-RH-P) and inhibits the rhythm-generating extensor neuron in the left shoulder pitch (E-LS-P). The rhythm-generating flexor neuron in the left hip (F-LH-P) excites the rhythm-generating extensor neuron in the right hip (E-RH-P) and inhibits the rhythm-generating flexor neuron in the left shoulder pitch (F-LS-P). The same synaptic excitation is proposed from the right hip to the left hip. For intra-limb circuitry, the rhythm-generating extensor neuron in the hip pitch (E-H-P) excites the rhythm-generating

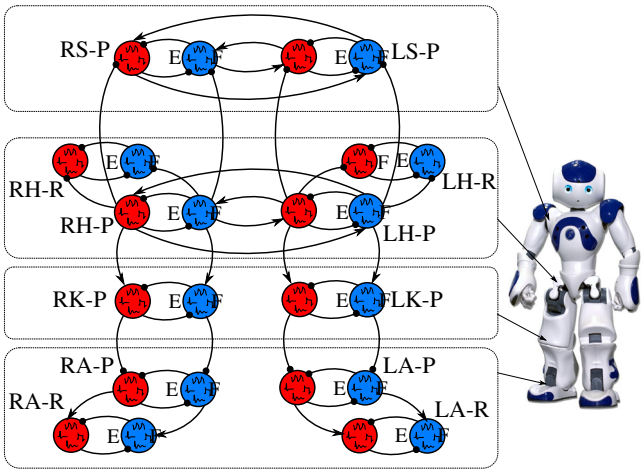

Fig. 7 Coupling circuitry between rhythm generator neurons. 'F' for flexion neuron and 'E' for extension neuron. RS-P and LS-P are right and left pitch shoulder rhythmic neurons. LH-P and LH-R are pitch and roll rhythmic neurons for the left hip. The other layers of each CPG are hidden for better readability of the figure

extensor neuron in the knee pitch (E-K-P) and inhibits the rhythm-generating extensor neuron in the hip roll (E-H-R) of the same leg. With this simple coupling, the robot can perform walking tasks from basic oscillatory patterns. These connections between rhythm generator neurons have been established manually by trial and error. However, a new coupling circuitry must be designed when addressing a new task. A desired task can be accomplished by defining its basic patterns and the related coupling circuit.

4.2 Synaptic connections and neuronal parameters

One of the important phases of the design of a CPG circuitry is the connection with feedback. Proprioception and exteroception feed the CPG neurons at different layers: rhythm-generation neurons, pattern-formation neurons, motoneurons, and interneurons (Rybak et al. 2006). Proprioception at a particular joint affects the corresponding motor neurons of the same joint (e.g., the extensor sensory neuron inhibits the extensor motor neuron of the same joint), and other joints' proprioception feeds motoneurons of other joints (e.g., the AS sensor neuron in Table 2 represents the effect of hip joint angle on the knee motor neuron) (Manoonpong et al. 2007). This section details the connectivity inside the CPG for each joint of the robot: shoulder pitch, hip pitch, hip roll, knee pitch, ankle pitch, and ankle roll.

All synaptic connections between RG neurons and in the coupling circuitry are fixed at 1, considering the polarity between them. All connections from RG neurons to PF neurons and all connections from PF neurons to MN neurons are also fixed at 1. Only the synaptic connections for the sensory feedback signals are designed manually to achieve a stable walking. These values would need to be redesigned for a different robotic platform. A reinforcement learning algorithm can be used to adjust the synaptic connections for the sensory feedback. Although it is not the focus of the current paper, in our previous work, we proposed an experience-based learning technique that learns in the space of intrinsic parameters of the walking controller (i.e., σ_s, the amplification of motor pitch and roll) (Nassour et al. 2009; Nassour et al. 2013).

The weights of the synaptic connections of the CPG of hip joint pitch, hip roll, shoulder pitch, and ankle roll are shown in Table 1. FS and ES are flexion and extension sensory neurons, respectively, from corresponding joints. The variation in the descending control σ_s and σ_f allows the CPG to produce different motion patterns (Plateau, Quiescent, Almost an Oscillator, and Oscillators with different frequencies), while the variation in the descending control α and θ allows the CPG to shape the generated patterns.

The weights of the synaptic connections of the CPG of knee-joint pitch are shown in Table 2. AS sensory neuron represents the stretch receptor for anterior extreme angle of the hips. In this work, the AS sensory neuron is represented

Table 1 Synaptic connections of the CPG for hip pitch, hip roll, shoulder pitch, ankle roll

Source	Target neuron					
	RG-E	RG-F	PF-E	PF-E	MN-E	MN-F
σ_s	[0,5]	[0,5]	–	–	–	–
σ_f	[0,5]	[0,5]	–	–	–	–
α	–	–	[0,∞]	[0,∞]	–	–
θ	–	–	[−∞, ∞]	[−∞, ∞]	–	–
RG-E	–	−1	1	–	–	–
RG-F	−1	–	–	1	–	–
PF-E	–	–	–	–	1	–
PF-F	–	–	–	–	–	1
ES	–	–	–	–	−0.4	–
FS	–	–	–	–	–	−0.4

Table 2 Synaptic connections for knee pitch CPG

Source	Target neuron					
	RG-E	RG-F	PF-E	PF-E	MN-E	MN-F
σ_s	[0,5]	[0,5]	–	–	–	–
σ_f	[0,5]	[0,5]	–	–	–	–
α	–	–	[0,∞]	[0,∞]	–	–
θ	–	–	[−∞, ∞]	[−∞, ∞]	–	–
RG-E	–	−1	1	–	–	–
RG-F	−1	–	–	1	–	–
PF-E	–	–	–	–	1	–
PF-F	–	–	–	–	–	1
ES	–	–	–	–	−0.4	–
FS	–	–	–	–	–	−0.4
AS	–	–	–	–	0.9	−0.9

Table 3 Synaptic connections for ankle pitch CPG

Source	Target neuron					
	RG-E	RG-F	PF-E	PF-E	MN-E	MN-F
σ_s	[0,5]	[0,5]	–	–	–	–
σ_f	[0,5]	[0,5]	–	–	–	–
α	–	–	[0,∞]	[0,∞]	–	–
θ	–	–	[−∞,∞]	[−∞,∞]	–	–
RG-E	–	−1	1	–	–	–
RG-F	−1	–	–	1	–	–
PF-E	–	–	–	–	1	–
PF-F	–	–	–	–	–	1
ES	–	–	–	–	−0.4	–
FS	–	–	–	–	–	−0.4
GB	–	–	−0.1	0.1	–	–
GF	–	–	0.1	−0.1	–	–
FB	–	–	−0.1	0.1	–	–
FF	–	–	0.1	−0.1	–	–

by the FS sensory neuron for the hip joint pitch. Based on AS, the hip flexion excites the knee extension motor neuron and inhibits the knee flexion motor neuron.

The weights of the synaptic connections of the CPG of ankle joint pitch are shown in Table 3. The exteroception sensory neurons GB and GF represent the effect of the ground contact sensor on the ankle joint. These neurons are tuned to match less than 0.1 (10 %) of the Sigmoid activation in the foot-swing phase, and they match 0.9 (90 %) of the Sigmoid activation for the foot-stance phase.

The exteroception patterns fall backward (FB) and fall forward (FF) represent the effect of the torso angle with the vertical direction on the ankle joint. When the torso bends forward (walking direction) and increases the angle with the vertical, the FF sensor neuron becomes more active. When the torso bends backward and increases the angle with the vertical, the FB sensor neuron becomes more active. These two neurons project to pattern-formation neurons of the ankle joint CPG.

4.3 Phase resetting

Walking is a periodic interaction between the robot and the environment that allows it to displace on the terrain to reach its requirements. However, an external disturbance can delay or advance its limit cycle's phase. Phase resetting is a technique by which the oscillation neurons phases were driven by external variables. In this study, we used ground contact sensory neurons to reset the rhythm generator neurons for all CPGs. The resetting is introduced by the injected current

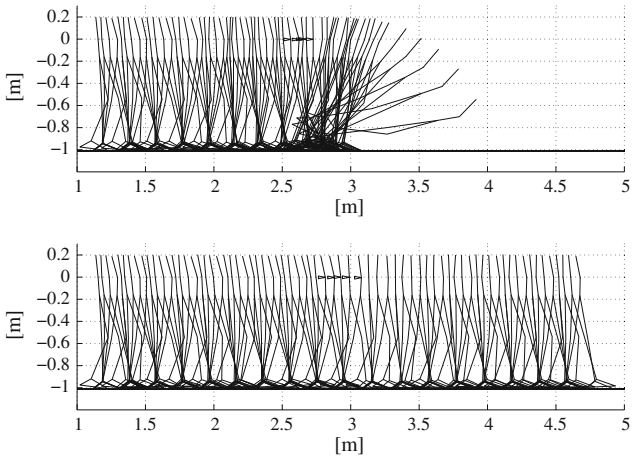

Fig. 8 *Upper* figure shows walking with oscillatory patterns without phase resetting, and the simulated walker falls after a disturbing force applied on the back during whole step. *Lower* figure shows walking and robustness to disturbances with phase resetting by ground

i_{inj} in Eq. (1). The injected current-related phase-resetting circuitry becomes active once the projection of the center of mass of the robot enters the support polygon of the landed foot. Figure 8 shows the role of the rhythm generator phase resetting subjected to a disturbing force of 10 N applied on the back of a simulated biped (22 Kg) during a whole step. The CPG architecture for the biped in Fig. 8 is similar to that presented in previous subsections.

In the first case, walking is achieved without phase resetting. In the second case, walking is achieved with phase resetting of the rhythm generator neurons, giving more robustness to the walking against the disturbing force. Of course, with a larger force, this technique cannot necessarily prevent the biped robot from falling, and other techniques can be employed under those circumstances.

5 Experimental and simulation results

This section presents experiments results on the use of the MLMP-CPG to control walking of a NAO humanoid robot.

To show the effectiveness of the proposed CPG model, we present two examples of rhythmic pattern generation, walking on flat terrain and walking on a sloped surface. To illustrate that stable walking was achieved, we provide a stability analysis in the case of flat terrain. We then present an example that combines rhythmic and non-rhythmic pattern while dealing with sudden external disturbance.

5.1 CPG to robot actuator

Because most humanoid robots are actuated with one motor for each degree of freedom, extension and flexion motoneurons' activities of the half-center CPG associate together in the motor command that drives the corresponding joint actuator.

The voltage of the joint motor is obtained similarly to that inside the model presented in Manoonpong et al. (2007):

$$V = M(U_E - U_F) \tag{15}$$

where V is input voltage of the motor, M is the amplification, and U_E and U_F are the output of extensor and flexor motor neurons (see Fig. 2).

In our case, the integration of the CPG outputs will be mapped to the humanoid robot actuated by one DC motor for each joint, which is controlled via a PID controller.

It is important to note that natural gait in humans is driven from multiple factors, including morphology, the number of effectors, and energy minimization (Cunningham et al. 2010). Furthermore, the effector for yaw rotation in the hip is not used in this study. For such reasons, the resulting walking gait is far from the natural gait in humans.

5.2 Rhythmic behaviors

In this section, we present two cases of rhythmic behaviors for walking on flat and sloped terrains, followed by a stability analysis.

5.2.1 Rhythmic behavior: walking on flat terrain

Rhythmic patterns have been employed to generate the periodic motion in walking. The motor coordination circuitry and the synaptic connections presented in the previous section have been taken into account (Sect. 4). The NAO humanoid robot showed stable walking behavior on flat terrain with speed of 0.1 m/s and step length of 7 cm. A video for walking is available on: http://web.ics.ei.tum.de/~nassour/naowalkingonflat.mp4.

5.2.2 Rhythmic behavior: walking on sloped terrain

To show the adaptation of the proposed CPG due to the descending control that adjusts its parameters, we performed sloped terrain walking. As in walking on flat terrain, rhythmic patterns are also employed for walking on sloped terrain. In the case of walking uphill, the flexion rhythm will dominate at the ankle joint, while the extension rhythm will dominate in case of walking downhill. This extension/flexion domination is driven by the descending control.

A high-level controller is required to adjust the descending control for pattern generation and pattern formation based on information from exteroception and proprioception. In this paper, the adjustment of the descending control (σ_s, σ_f,

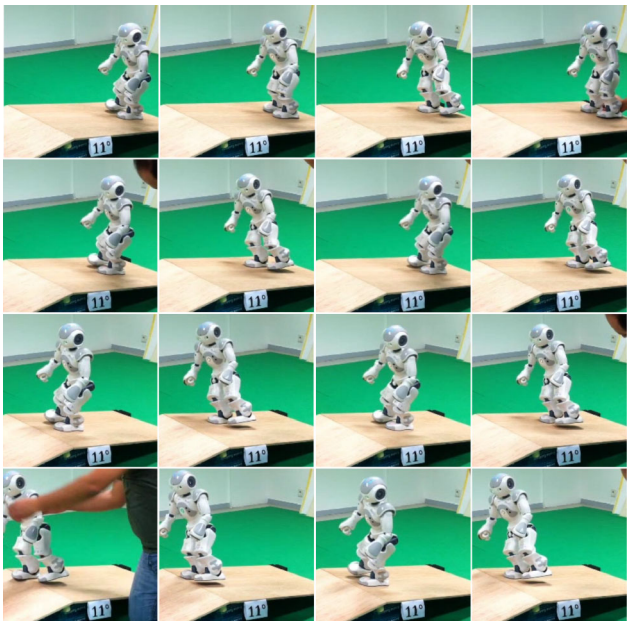

Fig. 9 Nao robot while walking uphill (a video is available on: http://web.ics.ei.tum.de/~nassour/naowalkinguphill.mp4).

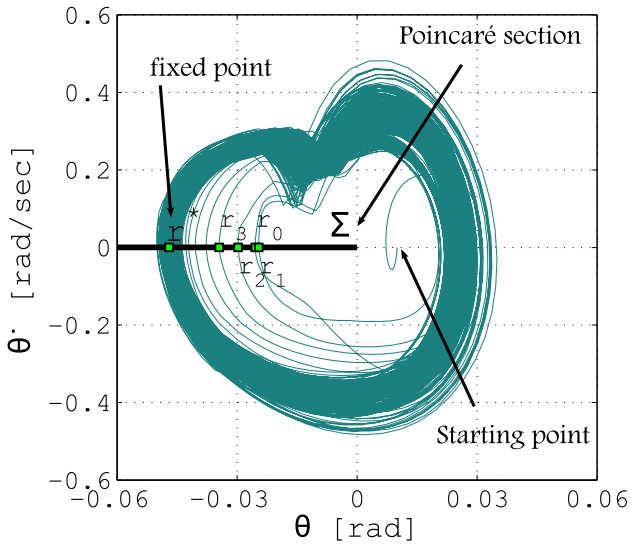

Fig. 10 Phase diagram of NAO robot torso inclination with the *Vertical* direction and stability analysis of the cycle based on Poincaré map

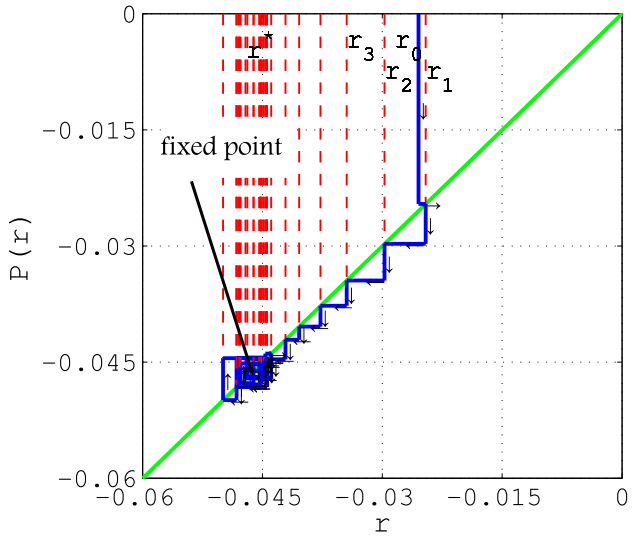

Fig. 11 Cobweb diagram for the sequence r_n given by Fig. 10

α_{MLR}, and θ_{MLR}) has been performed manually. In our other work, an experience-based learning mechanism has been proposed for learning meta-parameters of the central pattern generator (Nassour et al. 2013). Figure 9 shows snapshots of the NAO robot walking on terrain with an 11° upward slope. The amplitude of the oscillation is adjusted by varying the slope of the Sigmoid function in pattern-formation neurons (i.e., $\alpha_{\mathrm{MLR}} = -0.2$ for ankle joints). The center of oscillation in the joint is adjusted by varying the center point of the curve that denotes the threshold of the pattern-formation neuron (i.e., $\theta_{\mathrm{MLR}} = 0.15$ for ankle joints). The frequency of oscillatory patterns is tuned by the descending control for rhythm-generating neurons with σ_s and σ_f. Parameters of cycle timing and motoneuron activation are independently controlled; unlike the one-level CPG, this property provides a large range of control for walking on the slope with only a small number of parameters.

5.2.3 Stability analysis

To analyze the stability of the rhythmic motion during walking of the NAO robot regarding the dynamic interaction between the robot and the ground, we studied the phase diagram of the robot torso inclination with the vertical direction during a long walking period (250 s, 400 steps) (see Fig. 10).

Starting from initial position, this diagram shows the convergence of the walking cycle into a limit cycle. We are using Poincaré maps to study the swirling flows near the periodic orbit. We define $\sum$ as a transverse section on the flow in one direction with null velocity. The Poincaré map P is a mapping from $\sum$ to itself. Figure 11 shows first returns (r_0, r_1, r_2, r_3) approaching the limit cycle. A fixed point occurs at $r^* = 0.046$ where the cobweb diagram for the sequence r_n intersects the 45° diagonal line. The cobweb shows that the fixed point r^* is globally stable.

5.3 Non-rhythmic behavior: reaction against disturbance

This section highlights the employment of non-rhythmic patterns to respond to environmental changes. Figure 12 shows the pattern space for each joint of the NAO humanoid robot while switching from oscillatory patterns to non-oscillatory patterns to react to an external disturbing force applied at the

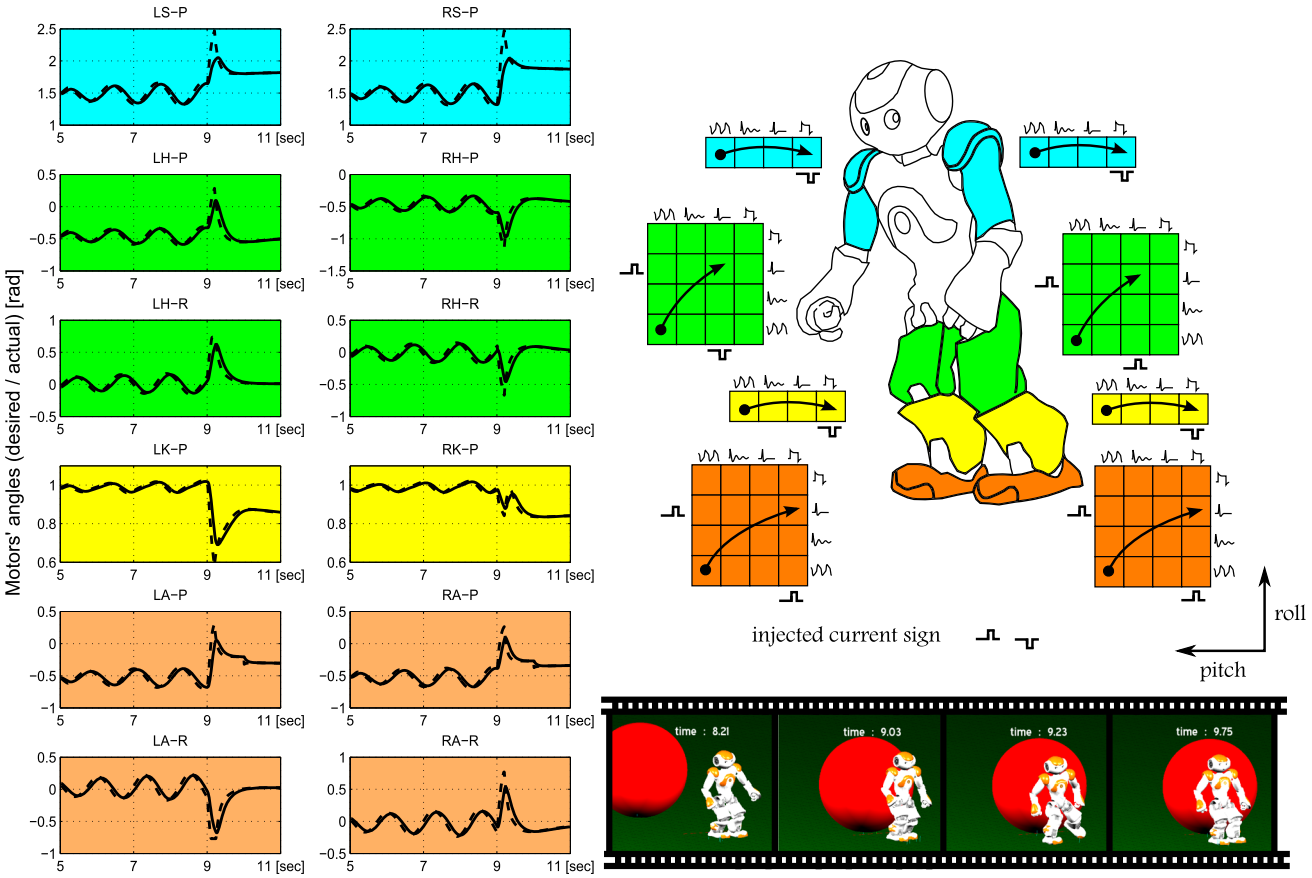

Fig. 12 NAO humanoid robot in simulation reacts against external disturbance by switching into another motor program on the pattern generation layer (a video is available on: http://web.ics.ei.tum.de/~nassour/naoballreactionsim.mp4.)

9th second during $t = 0.1$ s. This study was performed in the Webots simulator (www.cyberbotics.com). The disturbance comes from the collision with a ball that pushes the robot (robot mass is 4.3 Kg) from the back in the walking direction with a force of 34 N.

On the right-hand side, Fig. 12 illustrates the switching for each joint in the pattern space. On the left-hand side, the figure illustrates the switching in each joint with time. The direction of the switching in each joint is related to the direction of the injected current in the rhythm-generating neuron. The robot was performing walking behavior before the disturbance. Once the robot is subjected to the disturbance, the accelerometer output in the walking direction will exceed a predefined threshold, which triggers the switching into the designed recovery behavior. The two arms will move together to the back side by switching into the plateau motion pattern at each shoulder. Hip joints switch to the quiescent motion pattern with opposite direction for pitch joints and in the same direction for roll joints. Knee joints switch to the plateau motion pattern. Ankle joint pitch switches to the plateau motion pattern, while ankle joint roll switches to the quiescent motion pattern.

6 Conclusion

This paper presents a new central pattern generator model, named multi-layered multi-pattern CPG, which is able to generate a diverse range of motion patterns. Consistent with two neurophysiological studies, this CPG is based on three layers: rhythm-generation, pattern-formation, and motoneuron layers. At each layer, exteroceptive or proprioceptive afferent feedback can affect the shape or the frequency of the generated patterns, especially with phase resetting and phase shifting. The global circuitry based on this CPG is validated in the control of walking in a humanoid robot. Several simulations and experiments were carried out on the NAO humanoid robot. A Poincaré stability analysis showed that the walking was stable and the interaction with the environment flowed near a periodic orbit. The results showed that this neural circuitry is able to produce a 3D walking gait that remains stable when the slope of the ground changes and that can shift to another gait even when a sudden external force pushes the robot. Unlike previously proposed CPG models, the multi-layered multi-pattern CPG is able to produce behaviors that can combine both rhythmic and non-

rhythmic motion patterns within a single control framework. Such behavioral motions are essential for adaptive robot locomotion.

References

Amrollah E, Henaff P (2010) On the role of sensory feedbacks in rowat-selverston cpg to improve robot legged locomotion. Front Neurorobot 4:00113

Brown GT (1911) The intrinsic factors in the act of progression in the mammal. Proc R Soc Lond 84(572):308–319

Brown TG (1914) On the fundamental activity of the nervous centres: together with an analysis of the conditioning of rhythmic activity in progression, and a theory of the evolution of function in the nervous system. J Physiol 48(1):18–46

Choi JT, Bastian AJ (2007) Adaptation reveals independent control networks for human walking. Nat Neurosci 10(8):1055–1062

Cunningham CB, Schilling N, Anders C, Carrier DR (2010) The influence of foot posture on the cost of transport in humans. J Exp Biol 5(213):790–797

Degallier S, Righetti L, Gay S, Ijspeert A (2011) Toward simple control for complex, autonomous robotic applications: combining discrete and rhythmic motor primitives. Auton Robots 31(2–3):155–181

Endo G, Morimoto J, Matsubara T, Nakanishi J, Cheng G (2008) Learning cpg-based biped locomotion with a policy gradient method: application to a humanoid robot. Int J Robot Res 27:213–228

Endo G, Morimoto J, Nakanishi J, Cheng G (2004) An empirical exploration of a neural oscillator for biped locomotion control. In: Proceedings of the 2004 IEEE international conference on robotics and automation, ICRA 2004, April 26–May 1, 2004. LA, USA, New Orleans, pp 3036–3042

Geng T, Porr B, Wörgötter F (2006) Fast biped walking with a sensor-driven neuronal controller and real-time online learning. Int J Robot Res 25:243–259

Geyer H, Herr H (2010) A muscle-reflex model that encodes principles of legged mechanics produces human walking dynamics and muscle activities. IEEE Trans Neural Syst Rehabil Eng 18(3):263–273

Haken H, Kelso JAS, Bunz H, Haken H, Kelso JAS, Bunz H (1985) A theoretical model of phase transitions in human hand movements. Biol Cybern 51(5):347–356

Hoinville T (2007) Évolution de contrôleurs neuronaux plastiques : de la locomotion adaptée vers la locomotion adaptative. Ph.D. dissertation, University of Versailles St Quentin, Vélizy, France

Ijspeert AJ, Crespi A, Ryczko D, Cabelguen J-M (2007) From swimming to walking with a salamander robot driven by a spinal cord model. Science 315(5817):1416–1420

Koshland GF, Smith JL (1989) Mutable and immutable features of paw-shake responses after hindlimb deafferentation in the cat. J Neurophysiol 62(1):162–173

Lafreniere-Roula M, McCrea DA (2005) Deletions of rhythmic motoneuron activity during fictive locomotion and scratch provide clues to the organization of the mammalian central pattern generator. J Neurophysiol 94(2):1120–1132

Liu GL, Habib M, Watanabe K, Izumi K (2007) Cpg based control for generating stable bipedal trajectories under external perturbation. In: SICE, 2007 Annual conference, pp 1019–1022

Liu G, Habib M, Watanabe K, Izumi K (2008) Central pattern generators based on matsuoka oscillators for the locomotion of biped robots. Artif Life Robot 12(1):264–269

Manoonpong P, Geng T, Kulvicius T, Porr B, Wörgötter F (2007) Adaptive, fast walking in a biped robot under neuronal control and learning. PLoS Comput Biol 3(7):e134

Marder E, Bucher D (2001) Central pattern generators and the control of rhythmic movements. Curr Biol 11(23):R986–R996

Markin SN, Klishko AN, Shevtsova NA, Lemay MA, Prilutsky BI, Rybak IA (2010) Afferent control of locomotor cpg: insights from a simple neuromechanical model. Ann N Y Acad Sci 1198:21–34

Matsubara T, Morimoto J, Nakanishi J, aki Sato M, Doya K (2006) Learning cpg-based biped locomotion with a policy gradient method. Robot Auton Syst 54(11):911–920

Matsuoka K (1985) Sustained oscillations generated by mutually inhibiting neurons with adaptation. Biol Cybern 52(6):367–376

McCrea DA, Rybak IA (2008) Organization of mammalian locomotor rhythm and pattern generation. Brain Res Rev 57(1):134–146

Miyakoshi S, Taga G, Kuniyoshi Y, Nagakubo A (1998) Three dimensional bipedal stepping motion using neural oscillators-towards humanoid motion in the real world. Intelligent Robots and Systems. Proceedings., 1998 IEEE/RSJ international conference on, vol 1. IEEE, pp 84–89 (1998)

Nassour J, Henaff P, Ouezdou FB, Cheng G (2009) Experience-based learning mechanism for neural controller adaptation: application to walking biped robots. In 2009 IEEE/RSJ international conference on intelligent robots and systems, October 11–15, St. Louis, MO, USA, pp 2616–2621

Nassour J, Hugel V, Ouezdou F, Cheng G (2013) Qualitative adaptive reward learning with success failure maps: applied to humanoid robot walking. IEEE Trans Neural Netw Learn Syst 24(1):81–93

Orlovsky G, Deliagina T, Grillner S (1999) Neuronal control of locomotion from mollusc to man. Oxford University Press, Oxford

Perret C, Cabelguen J, Orsal D (1988) Stance and motion: facts and concepts. Plenum Press, New York, ch. Analysis of the pattern of activity in "knee flexor" motoneurons during locomotion in the cat, pp 133–141

Purves D, Augustine GJ, Fitzpatrick D, Hall WC, Lamantia A-S, McNamara JO, Williams SM (2004) Neuroscience, 3rd edn. Sinauer Associates Inc, Sunderland

Righetti L, Ijspeert AJ (2006) Programmable central pattern generators: an application to biped locomotion control. In: Proceedings of the 2006 iEEE international conference on robotics and automation, pp 1585–1590

Rossignol S, Dubuc R, Gossard J-P (2006) Dynamic sensorimotor interactions in locomotion. Physiol Rev 86(1):89–154

Rowat P, Selverston A (1991) Learning algorithms for oscillatory networks with gap junctions and membrane currents. Netw Comput Neural Syst 2(1):17–41

Rowat PF, Selverston AI (1997) Oscillatory mechanisms in pairs of neurons connected with fast inhibitory synapses. J Comput Neurosci 4(2):103–127

Rybak IA, Shevtsova NA, Lafreniere-Roula M, McCrea DA (2006) Modelling spinal circuitry involved in locomotor pattern generation: insights from deletions during fictive locomotion. J Physiol 577:617–639

Shik M, Orlovsky G, Severin F (1966) Organization of locomotor synergism. Biofizika 11(5):879–886

Shik ML, Severin FV, Orlovskiĭ GN (1966) Control of walking and running by means of electric stimulation of the midbrain. Biofizika 11(4):659–666

Swinnen SP, Vangheluwe S, Wagemans J, Coxon JP, Goble DJ, Impe AV, Sunaert S, Peeters RR, Wenderoth N (2010) Shared neural resources between left and right interlimb coordination skills: the neural substrate of abstract motor representations. NeuroImage 49(3):2570–2580

Taga G, Yamaguchi Y, Shimizu H (1991) Self-organized control of bipedal locomotion by neural oscillators in unpredictable environment. Biol Cybern 65(3):147–159

Wadden T, Ekeberg O (1998) A neuro-mechanical model of legged locomotion: single leg control. Biol Cybern 79(2):161–173